JOC Article
pubs.acs.org/joc

Tandem 1,5-Hydride Shift/1,5-S,N-Cyclization with Ethylene Extrusion of 1,3-Oxathiolane-Substituted Ketenimines and Carbodiimides. An Experimental and Computational Study†

Mateo Alajarin,* Baltasar Bonillo, Pilar Sanchez-Andrada, and Angel Vidal

Departamento de Quimica Organica, Facultad de Quimica, Universidad de Murcia, Campus de Espinardo, 30100 Murcia, Spain

alajarin@um.es

Received March 17, 2010

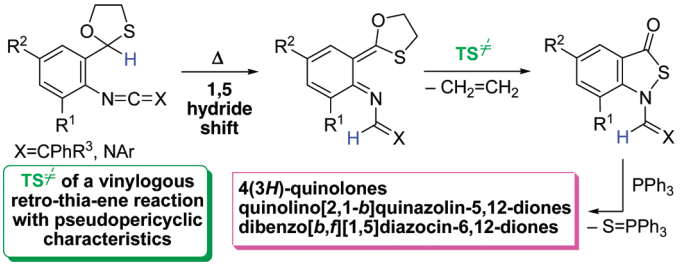

Under thermal activation in solution, *N*-[2-(1,3-oxathiolan-2-yl)]phenyl ketenimines and carbodiimides were converted into 2,1-benzisothiazol-3-ones bearing a pendant *N*-styryl or imidoyl fragment, respectively. These processes should occur with the concomitant formation of ethylene as result of the fragmentation of the 1,3-oxathiolane ring. The conversions of ketenimines took place under softer thermal conditions, toluene 110 °C, than those of carbodiimides, *o*-xylene 160 °C. A computational DFT study unveiled the mechanistic course of these transformations, rare tandem processes consisting of an initial 1,5-hydride shift of the acetalic hydrogen atom to the central carbon atom of the heterocumulene function leading to the respective *o*-azaxylylene. This transient intermediate then converts, in a single step, into ethylene and the experimentally isolated benzisothiazolone. This latter stage of the mechanism is rather peculiar, combining a 1,5-cyclization by S−N bond formation, aromaticity recovery at the benzene nucleus, and the fragmentation of the oxathiolane framework originating a new carbonyl group. It can be related with a vinylogous retro-ene reaction and shows pseudopericyclic characteristics. The computations also revealed that the alternative 6π electrocyclization of the transient *o*-azaxylylenes cannot compete, on kinetic and thermodynamic grounds, with the experimentally observed reaction channel. The two alternative reaction paths of a number of ketenimines and carbodiimides were computationally scrutinized, the results being in accord with the experimental outcomes. In addition, sulfur extrusion from the benzisothiazolones by the action of triphenylphosphine under two different reaction conditions led to three different types of heterocyclic products, 4(3*H*)-quinolones, quinolino[2,1-*b*]quinazolin-5,12-diones, and dibenzo[*b*,*f*][1,5]diazocin-6,12-diones, whose formation is explained by the initial formation of an intermediate imidoylketene. This reactive species could be trapped by a nucleophilic solvent, ethanol.

Introduction

Compounds typically classified as possessing *hydricity* (hydride donor ability) are predominantly metal hydrides, structural analogues of NADH and triarylmethane derivatives.[1]

In the course of investigations directed toward the finding of new compounds that may act as potential hydrogen storage materials, several covalent organic molecules have emerged as new organic hydrides, among them 1,3-dinitrogenated heterocyclic

† In memory of Prof. Jose M. Concellon, who recently passed away.

(1) Ellis, W. W.; Raebiger, J. W.; Curtis, C. J.; Bruno, J. W.; DuBois, D. L. *J. Am. Chem. Soc.* **2004**, *126*, 2738–2743.

DOI: 10.1021/jo100502p Published on Web 05/12/2010

SCHEME 1. Reaction Path Converting Ketenimines and Carbodiimides 1 into Quinolines and Quinazolines 3

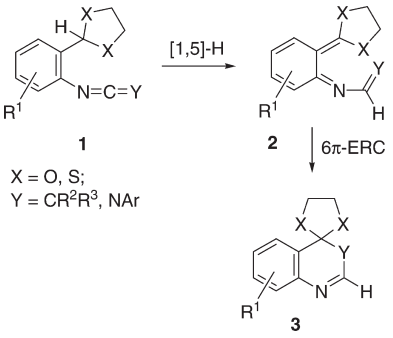

systems such as *N,N*-dimethylbenzimidazoles,[2] 2-benzoyl-*N,N*-dimethylperhydropyrimidine,[3] and orthoformamides.[4] However, no structurally related compounds bearing two oxygen or two sulfur atoms in relative 1,3 positions have been included into the class of compounds having hydricity. Exceptionally, the cationic polymerization of cyclic acetals has been proposed to be initiated by the transfer of a hydride from the acetalic carbon atom to the cationic initiator.[5]

While exploring new reactions of ketenimines,[6] we have recently found that *N*-[2-(1,3-dioxolan-2-yl)phenyl] ketenimines **1** (X = O; Y = CR^2R^3) and *N*-[2-(1,3-dithiolan-2-yl)phenyl] ketenimines **1** (X = S; Y = CR^2R^3), under thermal conditions, converted into spiroquinolines **3** (X = O, S; Y = CR^2R^3) by a tandem [1,5]-H migration/6π electrocyclic ring closure (6π-ERC) sequence involving the transient *o*-azaxylylenes **2** (Scheme 1).[7] The [1,5]-H shifts leading from acetal-(dithioacetal) ketenimines **1** to the intermediate azaxylylenes **2** were characterized as intramolecular *hydride transfers* from the acetalic functions to the electrophilic central carbon atom of the ketenimine moieties, on the basis of the weakening and polarization of the acetalic C−H bond by hyperconjugative interaction of its σ^*(C−H) orbital with the lone-pair electrons at the vicinal heteroatoms of the acetalic function. This assumption was confirmed by means of a computational DFT study, which also accounted for the modest activation energies of these hydride shifts, considerably lower than similar processes in the absence of the activating acetalic units. Thus, these results first demonstrated the hydricity-imparting character of the 2-monosubstituted 1,3-dioxolane and 1,3-dithiolane functions. Additionally, the experimental work and the computational calculations showed that the 1,3-dioxolane fragment activated more efficiently such [1,5]-H shifts than the thioanalogous 1,3-dithiolane functions.[7]

We also tested similar reactions involving carbodiimide functions as the termini of these hydride migrations. The cyclization of 1,3-dioxolane-carbodiimides **1** (X = O; Y = NAr) to spiroquinazolines **3** (X = O; Y = NAr), by a similar tandem process, required stronger reaction conditions than the analogous dioxolane-ketenimines. Furthermore, the 1,3-dithiolane-carbodiimides **1** (X = S; Y = NAr) were less reactive and could not be transformed into the putative spiroquinazolines **3** (X = S; Y = NAr) under a variety of thermal conditions.[7]

A logical next step of these investigations was to test the ability of 1,3-oxathiolane functions, another class of acetalic rings, to promote similar cyclizations. Herein we report our results on the thermal treatment of *N*-[2-(1,3-oxathiolan-2-yl)]-phenyl ketenimines and *N*-[2-(1,3-oxathiolan-2-yl)]phenyl-*N*′-aryl carbodiimides, which unexpectedly converted these heterocumulenes into 2,1-benzisothiazol-3-ones.[8] A computational DFT study will show that these transformations seem to occur via a formal [1,5]-H shift/1,5 electrocyclization/[3 + 2] cycloreversion tandem process, with the concomitant formation of ethylene. We here also disclose that sulfur extrusion from some of the so obtained 2,1-benzisothiazol-3-ones yields three types of heterocyclic products by the action of triphenylphosphine under two different reaction conditions.

Results and Discussion

The reaction of 2-azidobenzaldehydes **4** with 2-mercaptoethanol in the presence of *p*-toluenesulfonic acid as catalyst, in refluxing benzene, yielded the 2-(2-azidophenyl)-1,3-oxathiolanes **5** in good yields (86−99%). The Staudinger imination of triphenylphosphine with the azides **5**, in anhydrous diethyl ether at room temperature, provided the iminophosphoranes **6** (67−95%). The aza-Wittig reaction of compounds **6** with diphenylketene or methylphenylketene, in anhydrous toluene at room temperature, generated smoothly the *N*-[2-(1,3-oxathiolan-2-yl)]phenyl ketenimines **7**, which were used in the following step without further purification. After the toluene solutions containing ketenimines **7** were heated under reflux for a few hours, the 1-(β-styryl)-2,1-benzisothiazol-3-ones **8** were isolated from the crude reaction mixture in fair to good yields (Scheme 2, Table 1), instead of the quinolines **9** which could be presumably expected as resulting from a [1,5]-H/6π electrocyclic ring-closure tandem process.

The structural determination of 1-(β-styryl)-2,1-benzisothiazol-3-ones **8** was achieved following their analytical and spectral data and confirmed by X-ray diffraction of a monocrystal of compound **8a** ($R^1 = R^2 = H$; $R^3 = Ph$).[9] Benzisothiazolone **8e** ($R^1 = R^2 = H$; $R^3 = CH_3$) was isolated as a mixture of *E*/*Z* isomers, in a relative ratio close to 4:1. Both diastereoisomers ***E*-8e** and ***Z*-8e** could be separated by column chromatography, and their configurations were elucidated by means of NOESY experiments.

Following these initial experiments with ketenimines, we tested similar conversions involving the 1,3-oxathiolane-carbodiimides

(2) (a) Schwarz, D. E.; Cameron, T. M.; Hay, P. J.; Scott, B. L.; Tumas, W.; Thorn, D. L. *Chem. Commun.* **2005**, 5919–5921. (b) Lee, I.-S. H.; Jeoung, E. H. *J. Org. Chem.* **1998**, *63*, 7275–7279. (c) Montgrain, F.; Ramos, S. M.; Wuest, J. D. *J. Org. Chem.* **1988**, *53*, 1489–1492.

(3) Zhang, X.-M.; Bruno, J. W.; Enyinnaya, E. *J. Org. Chem.* **1998**, *63*, 4671–4678.

(4) Brunet, P.; Wuest, J. D. *J. Org. Chem.* **1996**, *61*, 2020–2026 and references cited therein.

(5) Penczek, S. *Makromol. Chem.* **1974**, *175*, 1217–1252 and references cited therein.

(6) For some of our previous works on ketenimines, see: (a) Alajarin, M.; Bonillo, B.; Marin-Luna, M.; Vidal, A.; Orenes, R.-A. *J. Org. Chem.* **2009**, *74*, 3558–3561. (b) Alajarin, M.; Bonillo, B.; Vidal, A.; Bautista, D. *J. Org. Chem.* **2008**, *73*, 291–294. (c) Alajarin, M.; Bonillo, B.; Sanchez-Andrada, P.; Vidal, A.; Bautista, D. *J. Org. Chem.* **2007**, *72*, 5863–5866. (d) Alajarin, M.; Ortin, M.-M.; Sanchez-Andrada, P.; Vidal, A. *J. Org. Chem.* **2006**, *71*, 8126–8139. (e) Alajarin, M.; Ortin, M.-M.; Sanchez-Andrada, P.; Vidal, A.; Bautista, D. *Org. Lett.* **2005**, *7*, 5281–5284. (f) Alajarin, M.; Vidal, A.; Ortin, M.-M. *Tetrahedron* **2005**, *61*, 7613–7621. (g) Alajarin, M.; Vidal, A.; Ortin, M.-M. *Org. Biomol. Chem.* **2003**, *1*, 4282–4292. (h) Alajarin, M.; Vidal, A.; Tovar, F.; Conesa, C. *Tetrahedron Lett.* **1999**, *40*, 6127–6130. (i) Alajarin, M.; Molina., P.; Vidal, A. *Tetrahedron Lett.* **1996**, *37*, 8945–8948.

(7) Alajarin, M.; Bonillo, B.; Ortin, M.-M.; Sanchez-Andrada, P.; Vidal, A. *Org. Lett.* **2006**, *8*, 5645–5648.

(8) For a preliminary communication, see: Alajarin, M.; Bonillo, B.; Sanchez-Andrada, P.; Vidal, A.; Bautista, D. *Org. Let.* **2009**, *11*, 1365–1368.

(9) For the X-ray structure of compound **8a** see ref 8.

SCHEME 2. Preparation of 2,1-Benzisothiazol-3-ones 8

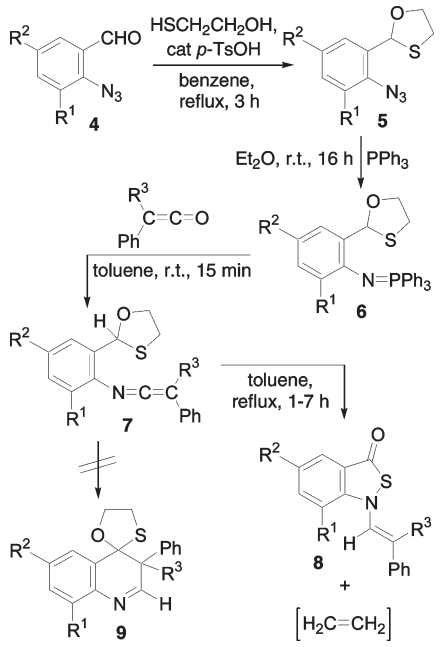

TABLE 1. 1-(β-Styryl)-2,1-benzisothiazol-3-ones 8

compd	R^1	R^2	R^3	yield (%)
8a	H	H	Ph	73
8b	CH_3	H	Ph	92
8c	H	Cl	Ph	74
8d	H	CH_3	Ph	92
8e	H	H	CH_3	81

10, easily synthesized from the iminophosphoranes **6** via aza-Wittig reaction with aryl isocyanates in anhydrous dichloromethane at room temperature. No conversion was observed while toluene or *o*-xylene solutions of carbodiimides **10** were heated at reflux temperature for several hours. We could accomplish the cyclization of carbodiimides **10** into the 1-(arylimino)methyl-2,1-benzisothiazol-3-ones **11** when *o*-xylene solutions of these heterocumulenes were heated at 160 °C in a sealed tube for 24 h (Scheme 3).

Taking into account the structures of the starting ketenimines **7** and carbodiimides **10** and those of the reaction products obtained in their thermal treatment, the cyclizations **7** → **8** and **10** → **11** should occur with the simultaneous formation of ethylene, although we did no efforts to ascertain the presence of this hydrocarbon in the gaseous exhausts of these reactions.

The presence of the hydrogen atom initially bonded to the acetalic carbon atom of the 1,3-oxathiolane function in ketenimines **7** and carbodiimides **10** at the styryl α-carbon atom of benzisothiazolones **8** and the iminic carbon atom of the 1-(arylimino)methyl substituent of benzisothiazolones **11**, respectively, suggests a [1,5]-H shift as the first mechanistic step for explaining the conversions **7** → **8** and **10** → **11**, leading to the transient *o*-azaxylylenes **12** (Scheme 4, R^1 and R^2 are omitted for simplicity). The formation of the final benzisothiazolones **8** and **11** from these azaxylylenes can be envisaged as occurring by a subsequent 1,5-electrocyclization via S−N bond formation leading to the sulfur ylides **13** (with its λ^4-S canonical ylene form **14**) followed by a final [3 + 2] cycloreversion at the 1,3-oxathiolane

SCHEME 3. Preparation of 2,1-Benzisothiazol-3-ones 11

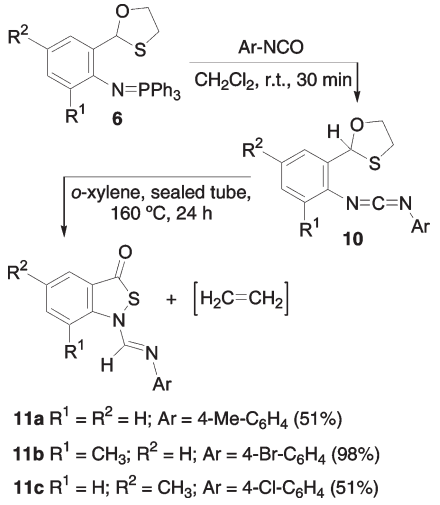

11a $R^1 = R^2 = H$; Ar = 4-Me-C_6H_4 (51%)

11b $R^1 = CH_3$; $R^2 = H$; Ar = 4-Br-C_6H_4 (98%)

11c $R^1 = H$; $R^2 = CH_3$; Ar = 4-Cl-C_6H_4 (51%)

SCHEME 4. Mechanistic Proposal for the Conversions 7 → 8 and 10 → 11

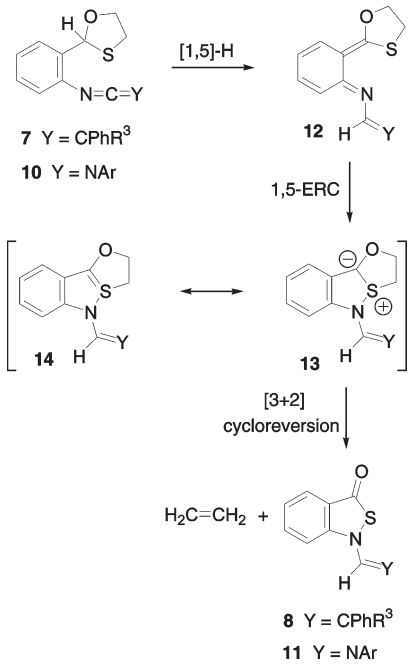

ring which would account for the fragmentation of **13** to ethylene and the experimentally isolated reaction products.

The first step of this mechanistic proposal is precedented in the Introduction. The two following steps merit some comments. Whereas the synthesis of isothiazole rings by S−N bond formation is not uncommon,[10] the practically unique protocol reported for the preparation of 2,1-benzisothiazole derivatives is the oxidation of *o*-aminobenzylthiols[11] and thioanthranilic acids.[12]

(10) Pain, D. L.; Peart, B. J.; Wooldridge, R. H. Isothiazoles and their Benzo Derivatives. In *Comprehensive Heterocyclic Chemistry*; Katritzky, A. R., Rees, C. W., Eds.; Pergamon Press: New York, 1984; Vol. 6, p 131.

(11) (a) Brown, D. W.; Sainsbury, M. *Sci. Synth.* **2002**, *11*, 573–626. (b) Davis, M. *Adv. Heterocycl. Chem.* **1972**, *14*, 43–98.

(12) (a) Böshagen, H.; Geiger, W. *Chem. Ber.* **1973**, *106*, 376–378. (b) Albert., A. H.; Robins, R. K.; O'Brien, D. E. *J. Heterocycl. Chem.* **1973**, *10*, 413. (c) Albert., A. H.; O'Brien, D. E.; Robins, R. K. *J. Heterocycl. Chem.* **1978**, *15*, 529–536.

SCHEME 5. Electronic Relationship between 15 and the Pentadienyl Anion 16

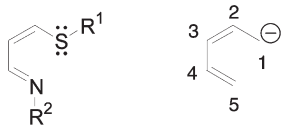

15 **16**

SCHEME 6. Conversion 17 → 19

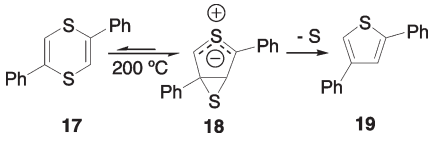

17 **18** **19**

No 6π-electrocyclization similar to the conversion **12** → **13** is, to our knowledge, previously known out of the plethora of 1,5-cyclizations.[13] In Huisgen's notation,[13b] the core nucleus **15** of this electrocyclization relates with the 6π-electron five-center carbon chain experiencing such a process, the pentadienyl anion **16**, by isoelectronic exchange of the carbanionic methylene by the sulfur atom and isoionic exchange of C5 by the iminic nitrogen atom (Scheme 5).

Only a scarce number of 1,5-electrocyclizations have been reported to convert neutral compounds into dipolar structures,[14] and in such cases, these latter species are commonly transient intermediates which, as in the present sequences **12** → **13** → **8**/**11**, transform further into neutral products through rearrangement or elimination reactions. A particularly pertinent and representative instance of such processes is the conversion of 1,4-dithiine **17** into thiophene **19** via the thiocarbonyl ylide **18**,[15] initially formed in small equilibrium concentration, which gains aromaticity by elimination of sulfur (Scheme 6). We believe that the electrocyclization **12** → **13** and the further dipolar cycloreversion[16] **13** → **8**/**11** may occur in a similar way, by combining the ring closure to the new five-membered ring with the departure of ethylene. The step **12** → **13** is associated with a change in the valence of the sulfur atom, by involvement of its empty 3d-orbitals, and the product **13** can be described by an ylidic resonance structure **13** and a neutral resonance form **14** with a hypervalent sulfur atom. Obviously, the recovery of the aromatic resonance energy at the benzene nucleus of **12** should decisively help to the ongoing cyclization step. As far as the third mechanistic step, the cycloreversion **13** → **8**/**11**, is concerned, and taking into account that the thioanalogues of intermediates **12**, structures **2** (X = S), have been shown to cyclize into quinolines **3** (X = S) instead of undergo a similar sequence to **12** → **13** → **8**/**11**, it seems clear that the generation of a strong C=O double bond in benzisothiazolones **8** and **11** should be decisive for the success of the prevailing reaction channel leading to these latter compounds.

SCHEME 7. Conversions of Compounds 20a−e into 21a−e and 22a−e plus Ethylene Approached in the Computational Study

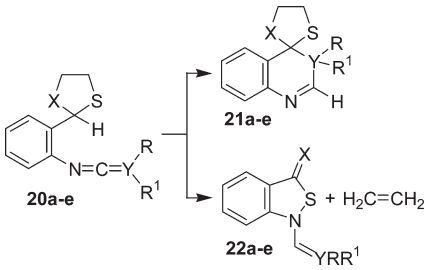

20a-e **21a-e** **22a-e**

The peculiarities of these two latter individual steps of our mechanistic proposal, converting the *o*-azaxylylenes **12** into the final benzisothiazolones **8**/**11**, and the striking differences experimentally found between the thermal behavior of dioxolane/dithiolane heterocumulenes **1** and that of their oxathiolane analogues **7** and **10**, led us to analyze more in depth the mechanistic sequence summarized in Scheme 4 by a detailed computational study.

Computational Study

In order to gain insight into the mechanistic path of the transformation of 1,3-oxathiolane-ketenimines **7** and 1,3-oxathiolane-carbodiimides **10** into ethylene plus the benzisothiazolones **8** and **11**, respectively, and also to answer why analogous 1,3-dithiolane-ketenimines did not experience a similar transformation, we have carried out a computational DFT study by using the model molecules depicted in Scheme 7.[17] We will discuss only the values of the calculated free energy barriers, unless otherwise stated.

First, we approached the transformation of the oxathiolane-ketenimine **20a** into the initially expected spiroquinoline **21a** and also into the benzisothiazolone **22a** (Scheme 7) resulting in the mechanistic paths shown in Figure 1. The first step, common to both reaction channels, consists of a [1,5]-H shift via transition structure **TS1a** leading to the intermediate *o*-azaxylylene ***Z*-23a**, which further can follow the two alternative pathways (a and b) depicted in Figure 1. Following path a, the *o*-azaxylylene ***Z*-23a** undergoes a 6π-electrocyclic closure through **TS2a** leading to spiroquinoline **21a**, whereas through path b, the azaxylylene *Z*→*E* isomerized its C1−N2 double bond, via transition state **TS3a**, converting ***Z*-23a** into its isomeric structure ***E*-23a**, which then is transformed into the benzisothiazolone **22a** plus ethylene. There is an alternative channel for the initial [1,5]-H shift involving the transition structure **TS1′a**, very close in energy to **TS1a**, which connects the oxathiolane ketenimine **20a** with the intermediate ***Z*-23′a**. This intermediate differs from ***Z*-23a** in the geometry around the C3−C4 double bond and can cyclize through transition state **TS2′a** to spiroquinoline **21a**, although, due to the geometry of the C3−C4 double bond, it cannot follow path b for conversion into benzisothiazolone **22a**. As the main electronic and energetic characteristics of **TS1′a**, ***Z*-23′a**, and **TS2′a** are very similar to those of **TS1a**, ***Z*-23a**, and **TS2a**, we will only comment on these latter structures.

(13) (a) Taylor, E. C.; Turchi, I. J. *Chem. Rev.* **1979**, *79*, 181–231. (b) Huisgen, R. *Angew. Chem., Int. Ed. Engl.* **1980**, *19*, 947–973. (c) George, M. V.; Mitra, A.; Sukumaran, K. B. *Angew. Chem., Int. Ed. Engl.* **1980**, *19*, 973–983. (d) Bakulev, V. A.; Kappe, C. O.; Padwa, A. In *Organic Synthesis: Theory and Applications*; Hudlicky, T., Ed.; JAI Press: Greenwich, 1996; Vol. 3, p 149.

(14) (a) Schultz, A. G.; DeTar, M. B. *J. Am. Chem. Soc.* **1976**, *98*, 3564–3572. (b) Wolf, T.; Waffenschmidt, R. *J. Am. Chem. Soc.* **1980**, *102*, 6098–6102. (c) Simmons, H. E.; Vest, R. D.; Blomstrom, D. C.; Roland, J. R.; Cairns, T. L. *J. Am. Chem. Soc.* **1962**, *84*, 4746–4756. (d) Beyer., H.; Bulka, E.; Beckhaus, F. W. *Chem. Rev.* **1959**, *59*, 2593–2599.

(15) Parham, W. E.; Traynelis, V. J. *J. Am. Chem. Soc.* **1954**, *76*, 4960–4962.

(16) Bianchi, G.; De Michaeli, C.; Gandolfi, R. *Angew. Chem., Int. Ed. Engl.* **1979**, *18*, 721–738.

(17) Although oxathiolane-ketenimine **20c** appears in the experimental study numbered as **7a**, for the sake of avoiding confusion we have used a different numbering system in the Computational Study section.

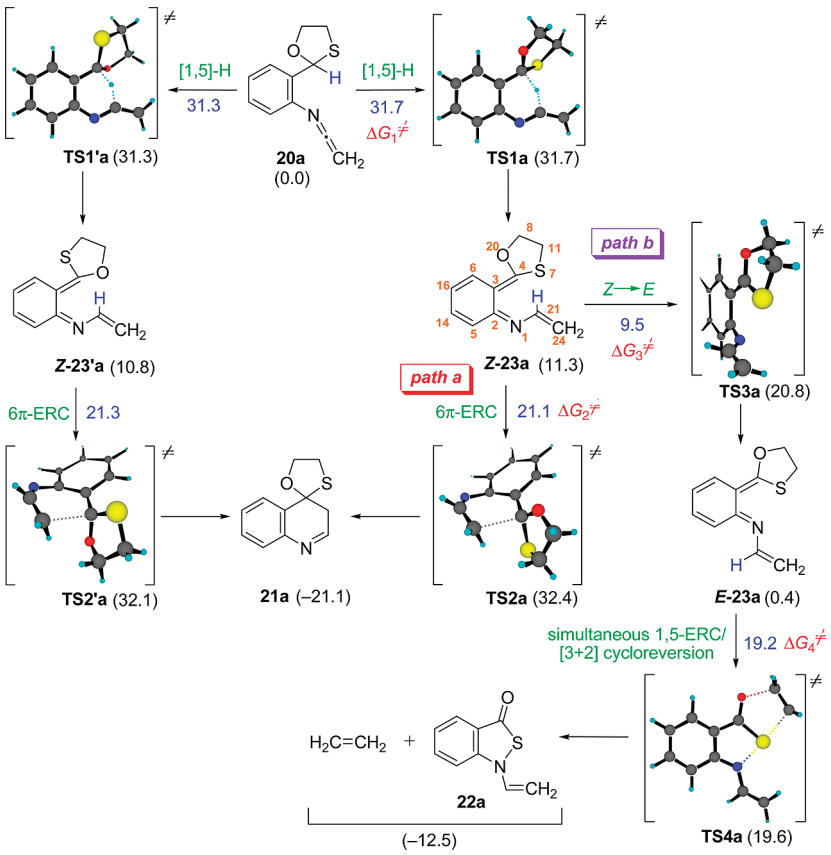

FIGURE 1. Stationary points optimized at the B3LYP/6-31+G** found in the transformation of the oxathiolane-ketenimine **20a** into the spiroquinoline **21a** and the benzisothiazolone **22a**. Numbers under the arrows correspond to free energies barriers in kcal·mol^{-1} calculated at the B3LYP/6-31+G** + ΔZPVE level. Numbers between parentheses correspond to relative free energies calculated at the same level.

The most relevant outcome of these calculations is that formation of benzisothiazolone **22a** plus ethylene does not involve a transient sulfur ylide similar to **13**; instead, *intermediate **E-23a** undergoes simultaneously the two previously postulated pericyclic events, 1,5-electrocyclization/[3 + 2] cycloreversion, via the transition state **TS4a***.

Concerning the first mechanistic step, the [1,5-H] shift converting **20a** into *o*-azaxylylene ***Z*-23a**, the calculated energy barrier (31.7 kcal·mol^{-1}) is similar to that previously found for the analogous [1,5]-H shift occurring in dioxolane-ketenimine **1** (X = O, Y = CH_2) (31.3 kcal·mol^{-1}),[7] showing that the hydricity of the 1,3-oxathiolane function is comparable to that of the 1,3-dioxolane function. This [1,5]-H shift can be described as a *hydride shift*, in which the acetalic C−H bond is weakened and polarized by the lone pairs at the O and S heteroatoms, inducing an increase of the negative charge density at the hydrogen atom.[4] Besides, the electrophilic nature of the central carbon atom of the ketenimine function[18] matches with the nucleophilic character of the migrating hydrogen.

The computed natural bond orbital (NBO) analysis of transition structure **TS1a** shows that the $n_X \rightarrow \sigma^*_{C-H}$ hyperconjugative interactions are the dominant among those involving the acetalic C−H bond [$n(2)_O \rightarrow \sigma^*_{C-H}$ = 11.69 kcal·mol^{-1}, $n(1)_S \rightarrow \sigma^*_{C-H}$ = 1.75 kcal·mol^{-1}, $n(2)_S \rightarrow \sigma^*_{C-H}$ = 5.35 kcal·mol^{-1}].[19] Besides, the analysis of the natural charges shows a significant increase of the sum of charges at the oxathiolane ring going from oxathiolane-ketenimine **20a** to the intermediate ***Z*-23a**, whereas this value decreases at the initial ketenimine fragment (Table 2).

TABLE 2. Sum of Natural Charges at the Oxathiolane and Ketenimine Fragments Calculated for the Stationary Points Found in the Conversion 20a → *Z*-23a

∑ charges	20a	TS1a[a]	*Z*-23a
oxathiolane ring	0.047	0.232	0.298
N−C−CH_2 fragment	−0.171	−0.024	−0.368

[a]For calculating the charge at the donor and acceptor carbon atoms C4 and C21 in **TS1a** we have considered the bond orders H−C4 and H−C21 and summed proportionally the charge of the migrating hydrogen atom into each carbon atom (see the atomic numbering in Figure 2).

On the other hand, we have found a noteworthy increase of the dipole moment going from **20a** (1.8 D) to **TS3a** (5.1 D) to ***Z*-23a** (5.9 D), accounting for the dipolar character of the intermediate ***Z*-23a**, with the negative charge delocalized over the aza-allylic system (N1−C21=C24), and the positive charge delocalized over the acetalic fragment (O−C4−S). It is also worth commenting on the helical geometry of this intermediate. The benzenoid ring of this polienic structure is not totally flat; the values of the C5−C2−C3−C6 and C1−C2−C3−C4 dihedral angles are 22.2° and 35.6°, respectively. In contrast, its geometric isomer ***E*-23a** is nearly planar, with only the C8−C20 ethylene fragment and the C21−C24 double bond departing from the plane containing the rest of the molecular framework. In addition, the calculated dipole moment of ***E*-23a** (3.9 D) is significantly lower than that found in ***Z*-23a**.

(18) Barker, M. W.; McHenry, W. E. In *The Chemistry of Ketenes, Allenes and Related Compounds*; Patai, S., Ed.; Wiley-Interscience: Chichester, UK, 1980; Part 2, p 701.

(19) It is known that the hyperconjugative interactions nx → σ*C-H involving lone pairs at the oxygen atoms are stronger than those involving sulfur atoms in analogous compounds. See: Alabugin, I. V. *J. Org. Chem.* **2000**, *65*, 3910−3919 and references cited therein.

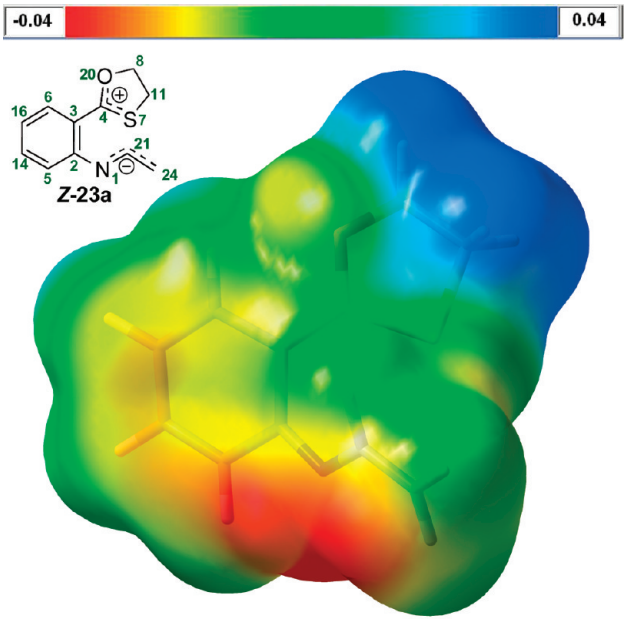

FIGURE 2. MESP of ***Z*-23a plotted onto the electron density surface with an isovalue of 0.01 au showing its highly polar character. The color coding is shown at the top.**

The dipolar nature of *o*-azaxylylene ***Z*-23a** can be also visualized by computing the molecular electrostatic potential (MESP) values, which are shown in Figure 2, reflecting the electron-rich and electron-deficient regions of the molecule.

In relation to the ring-closure step leading to spiroquinoline **21a**, we could not locate a rotational transition state connecting intermediate ***Z*-23a** with its *s-cis* rotamer along the N1−C21 bond required for the 6π electrocyclization. Instead, the IRC calculations showed that going uphill from intermediate ***Z*-23a** toward the transition structure **TS2a** the rotation around that single bond takes place gradually along with the partial formation of the new C4−C24 σ bond in the proximity of **TS2a**. The analysis of the geometry of this stationary point, the transition vector associated to its imaginary frequency and the intrinsic reaction coordinate (IRC) calculations point to a sort of disrotatory ring closure. The dipolar character of intermediate ***Z*-23a** may well facilitate this cyclization, as the ends of the 3-azahexatriene fragment are oppositely charged (natural charges at C4 and C24 are 0.22 and −0.02, respectively). The calculated energy barrier $\Delta G^{\ddagger}_{2}$ is 21.1 kcal·mol^{-1}, lower than that calculated for the archetypical 6π-electrocyclic ring closure of 1,3,5-hexatriene to 1,3-cyclohexadiene (27 kcal·mol^{-1}).[20]

Following path b, intermediate ***Z*-23a** first undergoes the *Z*→*E* isomerization of its C−N double bond through **TS3a**. This process occurs by a rotational mechanism, instead of the alternative inversion at the nitrogen atom, although the value of the C2−N1−C21 bond angle (135.1°) could reflect a minor contribution of inversional component to such isomerization mechanism. The increase of the dipole moment going from ***Z*-23a** (5.87 D) to **TS3a** (6.18 D), as well as the changes in the natural charges at the N1 atom (from −0.49 to −0.57) and the C2 atom (from 0.22 to 0.28) also illustrate the rotational nature of this *Z*→*E* isomerization.[21] The computed barrier for this step is very low, only 9.5 kcal mol^{-1}, and therefore easily surmountable.

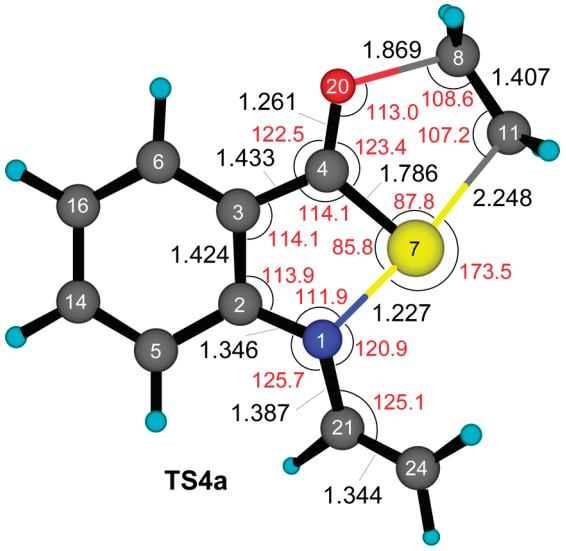

FIGURE 3. B3LYP/6-31+G**-optimized geometry of **TS4a** showing relevant bond distances (in Å) and bond angles (in deg).

Undoubtedly, the step along path b that called powerfully our attention was that converting intermediate ***E*-23a** into benzisothiazolone **22a** with simultaneous ethylene extrusion via the transition state **TS4a**, whose main geometric parameters are shown in Figure 3. This conversion can be formally viewed as the combination of two chemical events, a 1,5-electrocyclization and a [3 + 2] cycloreversion, into a single mechanistic step.

We have found in the literature neither 1,5-electrocyclizations of pentadienyl skeletons similar to the 1-thia-5-aza-2,4-pentadiene fragment of ***E*-23** nor [3 + 2] cycloreversions involving 1,3-oxathiolane rings like the one proposed above, and these two transformations do not look easily amenable in an isolated manner. Even so, the combination of both processes in a unique mechanistic step results in a process of a discrete energy barrier, close to 20 kcal·mol^{-1}. It seems that these two transformations cooperate in a favorable way by occurring simultaneously. Such cooperation may be interpreted by considering that the 1,5-electrocyclization might be viable thanks to the simultaneous ethylene extrusion, which probably occurs by virtue of the concurrent formation of the strong C=O bond, which in turn is favored by the S−N bond formation. Moreover, the aromaticity recovery at the benzene ring along the way to **22a** and the inherent entropic assistance of this mechanistic step must be also decisive factors for determining its success (see Figure 5).

The inspection of the geometry and some electronic parameters of the transition state **TS4a** revealed the especial characteristics of this structure. The three rings of **TS4a** are in the same plane; in fact, **TS4a** is nearly planar, and only the exocyclic C=C double bond attached to the nitrogen atom projects out of the molecular plane. The developing π system of ethylene and that of the remaining molecular frame are perfectly perpendicular, indicating that going backward from **22a** plus ethylene to **TS4a** the nonbonding lone pairs at the heteroatoms interact with the p orbitals at the ethylene carbon atoms. In accordance, the second-order perturbation analysis[22] along the IRC

(20) (a) Rodríguez-Otero, J. *J. Org. Chem.* **1999**, *64*, 6842–6848. (b) Jiao, H.; Schleyer, P. v. R. *J. Am. Chem. Soc.* **1995**, *117*, 11529–11535. (c) Evanseck, J. D.; Thomas, B. E., IV; Spellmeyer, D. C.; Houk, K. N. *J. Org. Chem.* **1995**, *60*, 7134–7141. (d) Jefford, C. W.; Bernardinelli, G.; Wang, Y.; Spellmeyer, D. C.; Buda, A.; Houk, K. N. *J. Am. Chem. Soc.* **1992**, *114*, 1157–1165. (e) Baldwin, J. E.; Reddy, V. P.; Schaad, L. J.; Hess, B. A. *J. Am. Chem. Soc.* **1988**, *110*, 8554–8555.

(21) Raban, M *Chem. Commun.* **1970**, 1415–1416.

(22) (a) Reed, A. E.; Weinstock, R. B.; Weinhold, F. *J. Chem. Phys.* **1985**, *83*, 735–746. (b) Reed, A. E.; Curtiss, L. A.; Weinhold, F. *Chem. Rev.* **1988**, *88*, 899–926. (c) Reed, A. E.; Schleyer, P. v. R. *J. Am. Chem. Soc.* **1990**, *112*, 1434–1445.

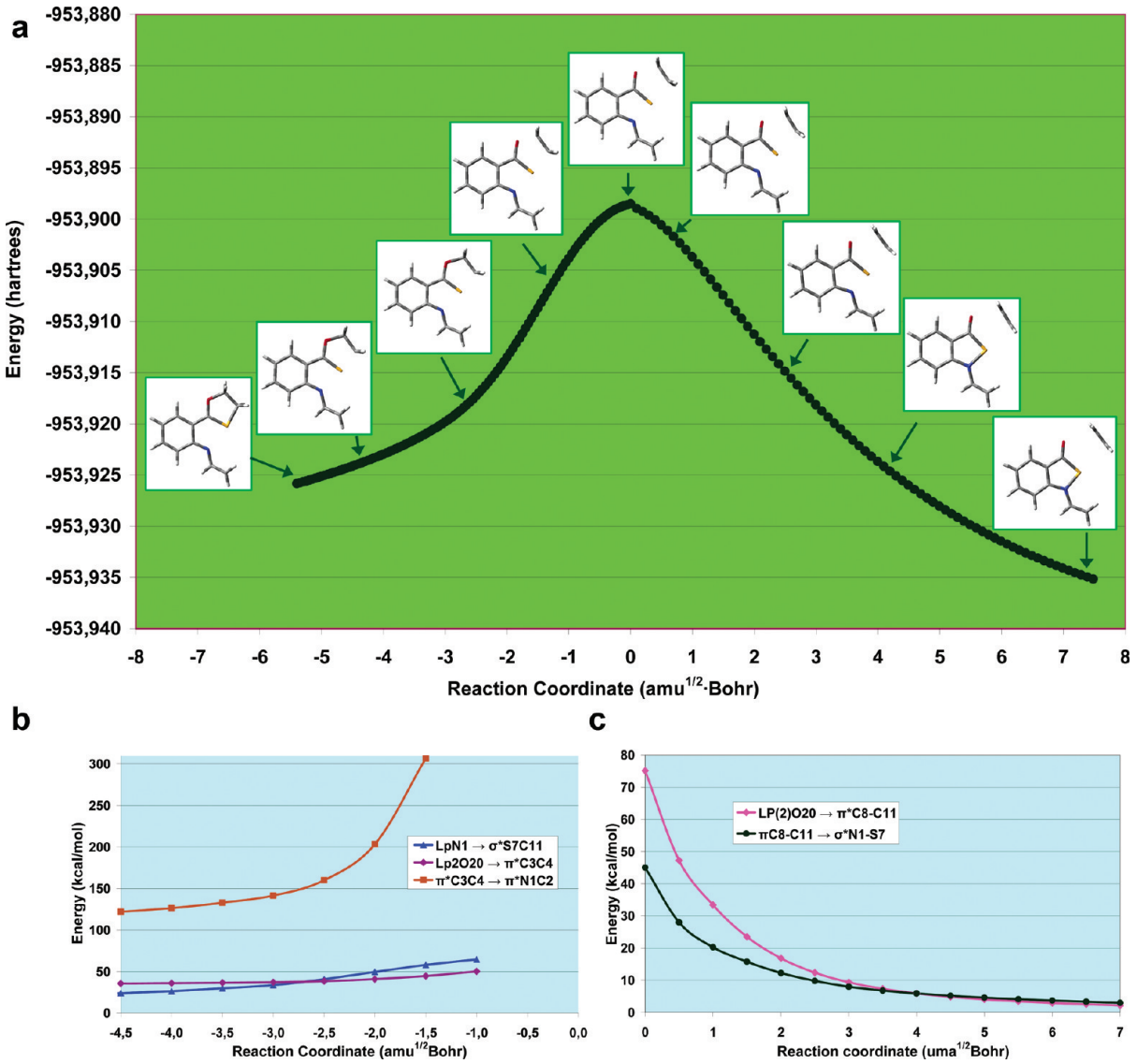

FIGURE 4. Main results of the second order perturbation analysis calculated for several points along the IRC calculations at the B3LYP/6-31+G** level of theory on **TS4a** (a), showing the relevant donor−acceptor interactions going forward from ***E*-23a to TS4a** (**b**) **and backward from 22a to TS4a** (**c**).

coordinate shows as the more relevant donor−acceptor interactions the $Lp_1O \rightarrow \pi^*C_8-C_{11}$ and $\pi C_8-C_{11} \rightarrow \sigma^*N-S$. As pointed out earlier, the geometry of the forming thiazole ring in **TS4a** does not correspond to that expected for a disrotatory 6π-electron five-center electrocyclization as all the atoms are in the molecular plane.[23] Going forward from ***E*-23a** to **TS4a**, the most relevant donor−acceptor interactions along the IRC are $LpN \rightarrow \sigma^*S-C_{11}$, $Lp_1O \rightarrow \pi^*C_3-C_4$ and $\pi^*C_3-C_4 \rightarrow \pi^*N-C_2$. The results of the IRC calculations for **TS4a** are shown in Figure 4.

Therefore, the electronic movements in the direct and inverse reaction paths passing through **TS4a** could be represented as shown in Figure 5. Accordingly, the planar geometry and the orbital topology of **TS4a**, containing orbital disconnections in the cyclic array of overlapping orbitals (where orthogonal bonding and nonbonding orbitals interchange roles), both confer pseudopericyclic[6e,24] characteristics to this transition state.

As the electronic reorganization only takes place at the periphery of **TS4a**, the single C4−S7 bond not intervening, the transformation of ***E*-23a** into **22a** could be also viewed as a particular case of vinylogous retro-thia-ene reaction (Figure 6) in which the enophile component is ethylene and the vinylogous ene partner is triheterosubstituted, the migrating atom being sulfur.

The vinylogous ene processes are scarcely known, and we could only locate two documents reporting on these kind of reactions.[25] It is not surprising that all-carbon vinylogous ene reactions are so rarely reported. Whereas they would involve, if concerted, cyclic transition states involving eight electrons, they

(23) Houk, K. N.; Li, Y.; Evanseck, J. D. *Angew. Chem., Int. Ed. Engl.* **1992**, *31*, 682–708 and references cited therein.

(24) (a) Ross, J. A.; Seiders, R. P.; Lemal, D. M. *J. Am. Chem. Soc.* **1976**, *98*, 4325–4327. (b) Birney, D. M. *J. Org. Chem.* **1996**, *61*, 243–251. (c) de Lera, A. R.; Alvarez, R.; Lecea, B.; Torrado, A.; Cossio, F. P. *Angew. Chem., Int. Ed.* **2001**, *40*, 557–561. (d) Birney, D. M. *Org. Lett.* **2004**, *6*, 851–854. (e) Jones, G. O.; Xuechen, L.; Hayden, A. E.; Houk, K. N.; Danishefsky, S. J. *Org. Lett.* **2008**, *10*, 4093–4096.

(25) (a) Gollnick, K.; Griesbeck, A. *Tetrahedron* **1984**, *40*, 3235–3250. (b) Maas, H.; Roeper, M. *Preparation of alkoxydodecatrienes and analogous by a vinylogous ene reaction.* BASF AG, Germany, DE, 1995069, A1 20001005; CAN **2000**, *133*, 281536.

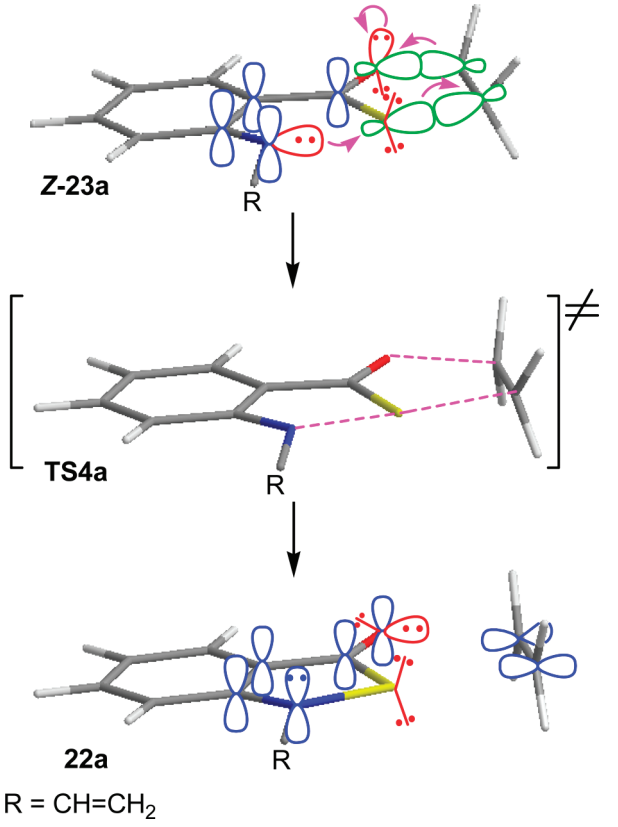

FIGURE 5. Proposed electronic reorganization going from ***Z*-23a to 21a through TS4a.**

could hardly compete with the alternative Diels−Alder reaction and other classical six-electron ene processes. Only the special structural and electronic features of the transformations ***E*-23** into **22** (heteroatoms, lone-pair interactions, pseudopericyclic character, and aromaticity recovery) seem to explain why these processes are easily amenable.

For the conversions **20b−e** into **21b−e**/**22b−e** we have only considered the [1,5]-H shift leading to the corresponding *o*-azaxylylenes ***Z*-23c-e**. The computations established the same mechanistic paths for the conversions of 1,3-dithiolane-ketenimine **20b**, 1,3-oxathiolane-ketenimine **20c**, and 1,3-oxathiolane-carbodiimides **20d−e** into the corresponding spiroquinolines **21b−e** and benzisothiazolones **22b−e**. However, the energy barriers calculated for these transformations are quite different as shown in Table 3. It is worth to stand out that the [1,5]-H shifts in oxathiolane-carbodiimides **20d,e** can take place via two alternative isomeric transition structures as result of the *trans* or *cis* geometry that the terminal C=N bond acquires at the end of those processes, leading to azaxylylenes ***trans*-*Z*-23d,e** and ***cis*-*Z*-23d,e**, respectively. As a consequence, these latter intermediates are converted into spiroquinolines **21d,e** via two alternative transition structures: **TS2**$_{out}$**d,e**, where the substituent at the terminal nitrogen atom is placed outward with relation to the σ C−N forming bond, and **TS2**$_{in}$**d,e**, where that substituent is placed inward. Moreover, in path b, the transformations of intermediates ***trans*-*Z*-23d,e** and ***cis*-*Z*-23d,e** into their corresponding geometrical isomers ***trans*-*E*-23d,e** and ***cis*-*E*-23d,e** occur via transition structures ***E*-TS3d,e** and ***Z*-TS3d,e**, respectively. Then these intermediates are transformed into the corresponding benzisothiazolones ***E*-** and ***Z*-22d,e** through the respective transition structures ***E*-TS4d,e** and ***Z*-TS4d,e**. This set of transformations is summarized in Scheme 8.

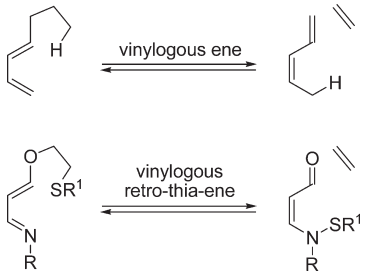

FIGURE 6. Vinylogous ene and retroene reactions and their analogy with a simplified model of the key mechanistic step leading to **22a**.

By analyzing the free energy barriers shown in Table 3 the following conclusions can be drawn:

1. In all cases the first step, the [1,5]-H sigmatropic shift, is predicted to be the rate limiting one.

2. By comparing the weights of the energy barriers calculated for the [1,5]-H shifts ($\Delta G^{\ddagger}_1$) in the transformations **20a,d** → ***Z*-23a,d** (entries 1 and 4), the decreasing predicted reactivity order is oxathiolane-ketenimine > oxathiolane-carbodiimide[26] and the comparison of the conversions **20a,b** → ***Z*-23a,b** (entries 1 and 2) shows that the [1,5]-H shift is easier in oxathiolane-ketenimine than in dithiolane-ketenimine. In other words, the hydride transfer occurs more easily in ketenimines than in carbodiimides, and the ability of the oxathiolane fragment for imparting hidricity is higher than that of the dithiolane function.

On the other hand, the substitution of hydrogen atoms by phenyl rings in the sp^2 carbon atom of the ketenimine function, or in the terminal nitrogen atom of the carbodiimide fragment, decreases the energy barrier associated at the [1,5]-H shift, as could be inferred by comparing the $\Delta G^{\ddagger}_1$ values of entries 1 and 3, those of entries 4 and 6, and those of entries 5 and 7. This behavior is probably due to the decrease in the energy of the LUMO orbital which takes place by substituting hydrogen atoms by benzene rings at the terminal atom of the heterocumulenic fragment.[27]

3. The 6π electrocyclic ring-closure step seems to be relatively easy in all cases. Thus, the calculated energy barriers associated to this step ($\Delta G^{\ddagger}_2$) are close to 20 kcal·mol^{-1} for the coversions ***Z*-23a,b** → **21a,b** and ***cis*-*Z*-20d,e** → **21d,e** (see entries 1, 2, 5, and 7). A significant increase in the barrier takes place when the hydrogens at the terminal carbon atom of the ketenimine moiety are substituted by phenyl groups, as revealed by comparing the $\Delta G^{\ddagger}_2$ values of entries 1 and 3. This fact can be rationalized on the basis of the higher steric interference of the two benzene rings in the transition structure **TS2c** when compared with the unsubstituted **TS2a**.[28]

Additionally, the computed energy barriers of the transformations ***trans*-*Z*-23d,e** → **21d,e** ($\Delta G^{\ddagger}_2$ in entries 4 and 6) are significantly lower than those associated to the remainder 6π electrocyclic ring closures. In particular, the barriers of the conversions ***trans*-*Z*-23d,e** → **21d,e** ($\Delta G^{\ddagger}_2$ in entries 4 and 6, around 4 kcal·mol^{-1}) are considerably lower than those of their

(26) The energy of the LUMO orbital of carbodiimide is higher than that of ketenimine; accordingly, it is expected that the donor−acceptor interaction between the migrating hydride and the heterocumulenic acceptor LUMO orbital should be less favorable in carbodimides than in ketenimines.

(27) It is known that conjugating substituents produce large accelerations of the rate of nucleophilic additions to heterocumulenes such as ketenes, see: Tidwell, T. T. *Ketenes*; J. Wiley and Sons: New York, 1995; p 581.

(28) (a) Marvel, E. N. In *Thermal Electrocyclic Reactions*; Academic Press: New York, 1980; Vol. 43, p 422. (b) Lewis, K. E.; Steiner, H. *J. Chem. Soc.* **1964**, 3080–3092. (c) Heller, H. G.; Salisbury, K. *J. Chem. Soc. C* **1970**, 399–402. (d) Spangler, C. W.; Jondahl, T. P.; Spangler, B. *J. Org. Chem.* **1973**, *38*, 2478–2484. (e) Marvell, E. N. *Tetrahedron* **1973**, *29*, 3791–3796. (f) Reid, P. J.; Doig, S. J.; Wickham, S. D.; Mathies, R. A. *J. Am. Chem. Soc.* **1993**, *115*, 4574–4763.

TABLE 3. Free and Electronic (in parentheses) Energy Barriers[a] (in kcal·mol^{-1}) for the Conversions 20a−e → 21a−c / (22a−e + Ethylene) Calculated at the B3LYP/6-31+G + ΔZPVE Theoretical Level**

entry	30 → 31/32	$\Delta G^{\ddagger}_1$	$\Delta G^{\ddagger}_2$	$\Delta G^{\ddagger}_3$	$\Delta G^{\ddagger}_4$	ΔG_{rxn21}	ΔG_{rxn22}	ΔG‡2
1	a	31.7 (29.9)	21.1 (20.2)	9.5 (9.2)	19.2 (19.1)	−21.1 (−23.4)	−12.5 (−9.6)	53.7 (53.9)
1′	a′	31.3 (29.3)	21.3 (20.4)			−21.1 (−23.4)		
2	b	33.3 (31.1)	21.1 (20.2)	10.4 (10.1)	27.5 (27.9)	−17.4 (−19.9)	1.9 (4.4)	53.1 (53.3)
3	c	26.9 (24.9)	26.4 (24.2)	9.5 (9.3)	20.5 (20.7)	−1.4 (−5.7)	−10.7 (−8.8)	36.2 (36.3)
4	d (*trans*)	37.4 (35.8)	4.0 (3.0)	4.1 (3.7)	16.8 (17.0)	−14.6 (−16.6)	−3.6 (−0.8)	41.6 (41.7)
5	d (*cis*)	36.7 (35.1)	21.0 (19.9)	4.9 (4.3)	18.7 (19.4)	−14.6 (−16.6)	−1.7 (1.3)	41.6 (41.7)
6	e (*trans*)	32.9 (30.8)	4.7 (3.3)	3.7 (3.2)	17.7 (21.4)	−8.3 (−10.8)	−4.9 (−2.4)	33.3 (33.2)
7	e (*cis*)	34.6 (32.8)	18.3 (16.4)	4.1 (3.5)	21.5 (17.8)	−8.3 (−10.8)	2.1 (4.7)	33.3 (33.2)

[a]See Figure 1 and Scheme 8 for the notation of the energy barriers.

SCHEME 8. Mechanistic Paths Found at the B3LYP/6-31+G Level for the Conversion of the Oxathiolane-Ketenimines 20d,e into Spiroquinolines 21d,e and Benzisothiazolones 22d,e plus Ethylene**

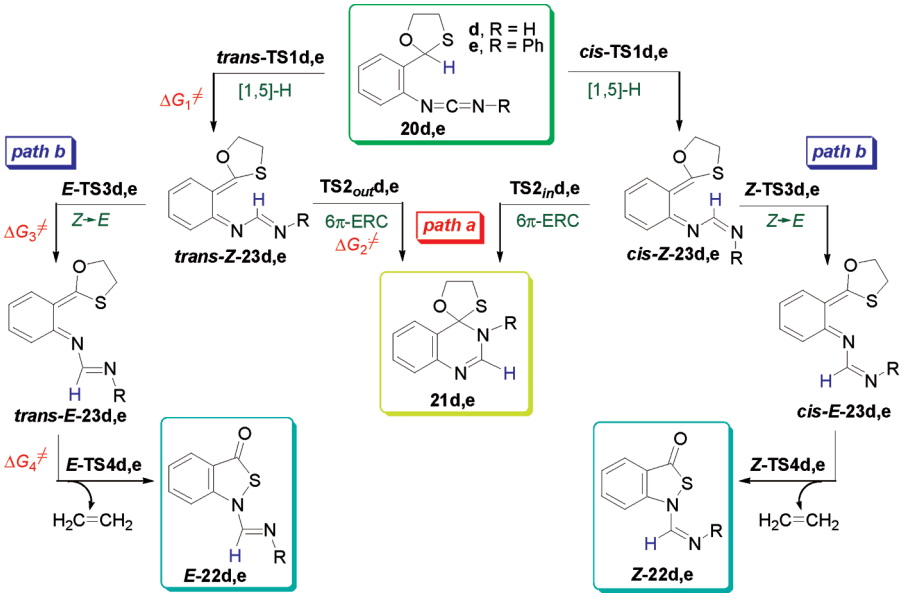

isomeric analogues ***cis-Z*-23d,e → 21d,e** ($\Delta G^{\ddagger}_2$ in entries 5 and 7, around 20 kcal·mol^{-1}). The assistance of the lone pair at the terminal heteroatom of ***trans-Z*-23d,e** to the formation of the new bond in the electrocyclization step can account for these differences. A similar assistance is not feasible in the cyclizations of ***cis-Z*-23d,e** given the geometry of the terminal C=N bond, as shown in Figure 7, where the transition structures of both transformations in case **d** are represented. In fact, the analysis of the second order perturbative interactions displayed in the NBO computations shows that the dominant orbital interactions in **TS2a-c** and **TS2$_{in}$d,e** take place between the C3=C4 and C21=Y24 π systems (see atomic numeration in Figure 7), as expected for a classical pericyclic disrotatory process. In contrast, in **TS2$_{out}$d,e** those interactions do not exist or are insignificant when compared with the dominant interaction $LpY_{24} \rightarrow \pi^*C_3{=}C_4$. Therefore, in these latter transitions states the assistance of the lone pair at the Y heteroatom of the hexatrienic fragment to the formation of the new σ bond, confers pseudopericyclic characteristics to the electrocyclizations of ***trans-Z*-23d,e** via **TS2$_{out}$d,e**. Similar 6π electrocyclic ring closures have been previously reported, and their characterization as pericyclic or pseudopericyclic process have been the object of several studies.[24c,29]

4. Concerning path b, the *Z* → *E* isomerization of the C2=N1 bond takes place via the transition structures **TS3a-e** involving the rotation around this bond, and in all cases these processes should occur very easily due to the small values of the computed energy barriers (0.5−10.2 kcal·mol).

5. As far as the conversion of *o*-azaxylylenes ***E*-23a-e** into the benzisothiazolones **22a−e** plus ethylene, through transition structures **ET4a-e** are concerned, the magnitudes of the energy barriers point out that these transformations are viable in all the studied cases, being more feasible for azaxylylenes bearing an oxathiolane ring ($\Delta G^{\ddagger}_4$ = 17.7−21.5 kcal·mol^{-1}) than for the dithiolane ($\Delta G^{\ddagger}_4$ = 27.5 kcal·mol^{-1}).

6. By comparing the relative values of the **20** → **21** and **20** → **22** reaction energies ($\Delta G^{\ddagger}_{rxn21}$ and $\Delta G^{\ddagger}_{rxn22}$, respectively), the calculations predict that in the conversion of **20a,b,d,e** the spiroquinolines **21a,b,d,e** should be the thermodynamically controlled product, whereas in the transformation of **20c** the benzisothiazolone **22c** should be both the thermodynamic and kinetically controlled product. At this point, it is worth comparing the reaction energy computed for the transformation of oxathiolane-ketenimine **20a** into **22a** ($\Delta G^{\ddagger}_{rxn22}$ = −12.5 kcal·mol^{-1}) with that of its thioanalogue, the conversion of dithiolane-ketenimine **20b** into **22b** ($\Delta G^{\ddagger}_{rxn22}$ = 1.9 kcal·mol^{-1}). This large difference presumably arises from the thermodynamically favorable generation of a strong C=O double bond in the

(29) (a) De Lera, A. R.; Cossio, F. P. *Angew. Chem., Int. Ed.* **2002**, *41*, 1150–1152. (b) Rodriguez-Otero, J.; Cabaleiro-Lago, E. M. *Chem.—Eur. J.* **2003**, *9*, 1837–1843. (c) Alajarin, M.; Sanchez-Andrada, P.; Cossío, F. P.; Arrieta, A.; Lecea, B. *J. Org. Chem.* **2001**, *66*, 8470–8477. (d) Alajarin, M.; Sanchez-Andrada, P.; Vidal, A.; Tovar, F. *J. Org. Chem.* **2005**, *70*, 1340–1349. (e) Alajarin, M.; Vidal, A.; Sanchez-Andrada, P.; Tovar, F.; Ochoa, G. *Org. Lett.* **2000**, *2*, 965–968. (f) Sakai, S. *Theor. Chem. Acc.* **2008**, *120*, 177–183. (g) Duncan, J. A.; Calkins, D. E. G.; Chavartha, M. *J. Am. Chem. Soc.* **2008**, *130*, 6740–6748.

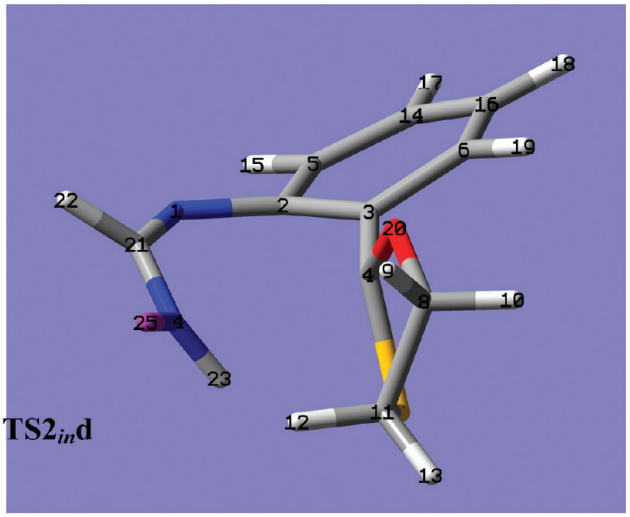

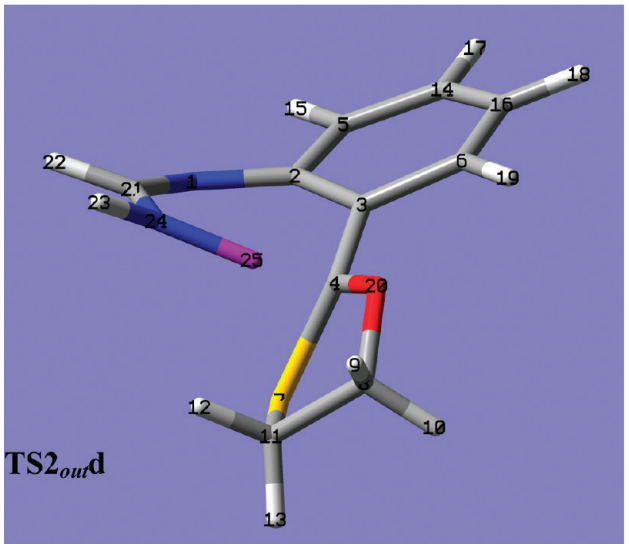

FIGURE 7. Stick representation of the B3LYP/6-31+G**-optimized geometries of the transition states **TS2$_{in}$d** and **TS2$_{out}$d** showing the lone pair (in purple, numbered as 25) at the terminal nitrogen atom.

benzisothiazol-3-one **22a** in comparison with the weaker C=S bond of the benzisothiazole-3-thione **22b**.

7. With the aim of correlating the results of the computational study with those of the experimental work, it is essential to compare the magnitude of the energy barriers computed for the 6π electrocyclic ring closure ($\Delta G^{\ddagger}_{2}$) with those of the key step of path b ($\Delta G^{\ddagger}_{4}$), but also the reaction energies $\Delta G^{\ddagger}_{\mathrm{rxn21}}$ and $\Delta G^{\ddagger}_{\mathrm{rxn22}}$, and to evaluate the potential reversibility of each step involved in these transformations. The key steps leading to the benzisothiazolones **22** are irreversible processes because of the accompanying ethylene extrusion, whereas the spiroquinolines **21** could revert into their corresponding azaxylylenes ***Z*-23** when the energy differences between **TS2** and **21** ($\Delta G^{\ddagger}_{-2}$) are affordable. Then, the benzisothiazolones **22** would be the predictable reaction products in those cases where: (a) $\Delta G^{\ddagger}_{4}$ is lower than $\Delta G^{\ddagger}_{2}$, as in the case of the transformations of **20a,c** and **20d** (entries 1, 3, and 5), and (b) $\Delta G^{\ddagger}_{2}$ is lower than $\Delta G^{\ddagger}_{4}$ but the spiroquinolines **21** can revert into the azaxylylenes ***Z*-23** ($\Delta G^{\ddagger}_{-2}$ is surmontable), and the corresponding $\Delta G^{\ddagger}_{4}$ energy barriers are also reachable. This could be the case of the conversion of **20e** (entries 6 and 7).

SCHEME 9. Sulfur Elimination in Benzisothiazolones and Isothiazolones

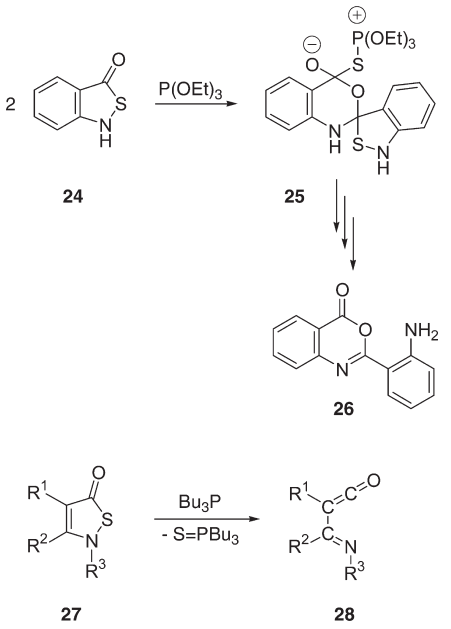

In contrast, if $\Delta G^{\ddagger}_{2} \ll \Delta G^{\ddagger}_{4}$ and the spiroquinolines **21** can not easily revert into ***Z*-23** (high $\Delta G^{\ddagger}_{-2}$ values), it is predictable that only the spiroquinolines **21** are obtained, as in the case of the conversion of **20b** and **20d** (entries 2 and 4). All these predictions agree with the experimental results. Note that the thermal treatment of the oxatiolane-ketenimine **7a** (which in the computational study appear as **20c**) and the oxathiolane-carbodiimide **10b** (whose structure is very similar to **20e**) led exclusively to the formation of benzisothiazolones **8a** and **11a**, respectively, whereas 1,2-dithiolane-ketenimines under thermal conditions were converted into the corresponding spiroquinolines (see ref 7), in agreement with the predictions of this computational study.

Desulfurization of Benzisothiazolones 8

Among the papers we located in a bibliographic search of synthetic methods and reactivity of benzisothiazolones, the one by Davis and co-workers[30] captured our attention. This paper reports on the sulfur extrusion from benzisothiazolone **24** by treatment with triethyl phosphite to yield 2-(2-aminophenyl)-4*H*-3,1-benzoxazin-4-one **26** (Scheme 9). The authors propose that the mechanistic course of the conversion **24** → **26** should occur by the initial formation of intermediate **25**, in which two molecules of benzisothiazolone and the phosphorus reagent coupled to form a unique dipolar species. Following an exhaustive literature search on the chemistry of heterocyclic systems structurally related to benzisothiazolones we located a second interesting publication, this one due to Goerdeler and co-workers,[31] disclosing a related desulfurization process of the most simple isothiazol-5(2*H*)-ones **27**, which provided imino-ketenes (imidoyl-ketenes) **28** as the initial reaction products, which were further reacted with nucleophilic reagents for yielding a variety of carbonyl derivatives.

(30) Davis, M.; Hook, R. J.; Wu, W. Y. *J. Heterocycl. Chem.* **1984**, *21*, 369–373.
(31) Goerdeler, J.; Yunis, M. *Chem. Ber.* **1985**, *118*, 851–862.

SCHEME 10. Desulfurization of 2,1-Benzisothiazol-3-ones 8

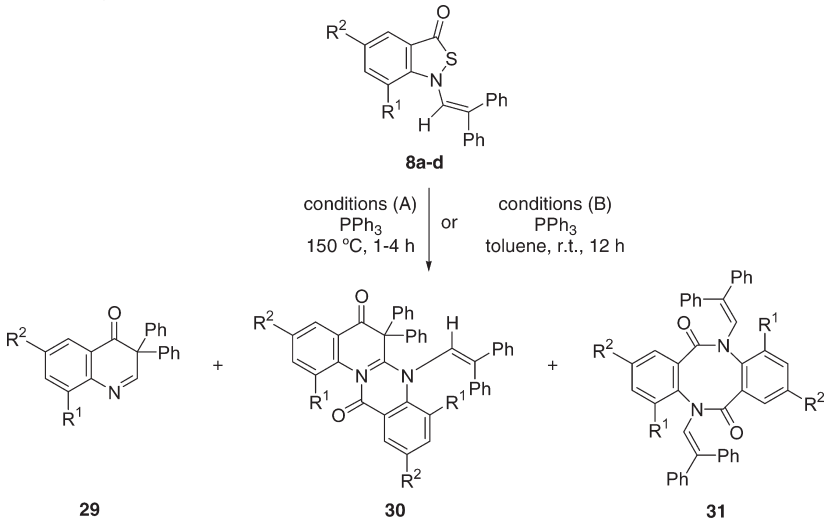

While the intermediacy of dipolar species **25** seemed to us somewhat unlikely, we envisaged that the formation of **26** could be more reasonably explained by a [4 + 2] dimerization of an intermediate imidoyl-ketene, benzoanalogue of **28**, which would result from the initial desulfurization of **24** by the action of the thiophilic phosphorus reagent, as occur with isothiazolones **27**. This reasoning directed our interest to the study of similar desulfurization processes of the herein obtained benzisothiazolones **8**, taking into consideration that the alkenyl chain linked to the N atom of **8** could result involved in intramolecular processes at the stage of the putative imidoyl-ketene intermediates.

The first reaction conditions we essayed involved the heating at 150 °C, in a sealed tube for 1−4 h, of equimolecular amounts of some benzisothiazolones **8** and triphenylphosphine. Under these conditions (A) compounds **8a** and **8d** converted into mixtures of the 3,3-diphenyl-4(*3H*)-quinolones **29a,d** and the quinolino[2,1-*b*]quinazolin-5,12-diones **30a,d**, the 4(*3H*)-quinolone **29b** being the only reaction product when starting from benzisothiazolone **8b**. Under softer reaction conditions, stirring toluene solutions of benzisothiazolones **8** and triphenylphosphine at room temperature for 12 h, conditions (B), benzisothiazolone **8b** converted into quinolone **29b**, compound **8c** transformed into dibenzodiazocindione **31c**, and **8d** afforded a mixture of quinolone **29d** and dibenzodiazocindione **31d** (Scheme 10 and Table 4).

The formation of the three types of desulfurization products **29**, **30**, and **31** could be reasonably explained by assuming the initial formation of the common transient imidoyl-ketene intermediates **32** (Scheme 11). The desulfurization of benzisothiazolones **8** by the action of triphenylphosphine should provide the very reactive species **32** bearing a 5-aza-1-oxa-1,2,4,6-heptatetraene system. The cyclization of intermediate **32** by a 6π-electron electrocyclic ring closure involving the C2−C3−C4−N5−C6−C7 azatriene fragment would then afford the 4(3*H*)-quinolones **29**. Thus formed compounds **29** could further undergo a [4 + 2] cycloaddition, acting as the dienophilic component across their endocyclic C=N bond, with a second molecule of imino-ketene **32** as the dienic partner, through its C2−C3−C4−N5 1-azadiene fragment, for yielding the quinolinoquinazolindiones **30**. Alternatively, the dibenzodiazocindiones **31** should form by coupling two molecules of **32** in a [4 + 4]-cycloadditive dimerization.

TABLE 4. Compounds 29−31

				yield (%)		
compd **8**	reaction conditions[a]	R^1	R^2	**29**	**30**	**31**
8a	A	H	H	27	60	
8b	A	CH_3	H	83		
8b	B	CH_3	H	99		
8c	B	H	Cl			53
8d	A	H	CH_3	28	47	
8d	B	H	CH_3	20		79

[a]See main text and Scheme 10.

The formation of products **29**, **30**, and **31** is in accordance with the known reactivity of imidoyl-ketenes, which have been shown to undergo 6π electrocyclic ring closures,[32] [4 + 2] cycloadditions[33] and dimerization through [4 + 4] cycloadditions.[34]

In general, under both reaction conditions quinolones **29** are formed in the product mixtures, with the rare exception of the desulfurization of **8c** under conditions B (Table 4). Compounds **30** are usually the major products when the reactions are run under reaction conditions A, whereas [4 + 4] cyclodimers **31** were only obtained under conditions B. The exclusive formation of quinolone **29b** in the two experimental desulfurization reactions of 2,1-benzisothiazolone **8b** ($R^1 = CH_3$; $R_2 = H$) can be rationalized by the steric influence of the methyl group $R^1 = CH_3$ at the *ortho* position of the iminic carbon atom in the imidoyl-ketene intermediate

(32) (a) Kappe, C. O.; Kollenz, G.; Wentrup, C. *J. Chem. Soc., Chem. Commun.* **1992**, 485–486. (b) Clarke, D.; Mares, R. W.; McNab, H. *J. Chem. Soc., Chem. Commun.* **1993**, 1026–1027. (c) Clarke, D.; Mares, R. W.; McNab, H. *J. Chem. Soc., Perkin Trans. 1* **1997**, 1799–1804. (d) George, L.; Netsch, K.-P.; Penn, G.; Kollez, G.; Wentrup, C. *Org. Biomol. Chem.* **2006**, *4*, 558–564.

(33) (a) Lisovenko, N. Y.; Krasnykh, O. P.; Aliev, Z. G.; Vostrov, E. S.; Tarasova, O. P.; Maslivets, A. N. *Chem. Heterocycl. Compd.* **2001**, *37*, 1314–1316. (b) Lisovenko, N. Y.; Maslivets, A. N.; Aliev, Z. G. *Chem. Heterocycl. Compd.* **2003**, *39*, 132–134. (c) George, L.; Bernhardt, P. V.; Netsch, K.-P.; Wentrup, C. *Org. Biomol. Chem.* **2004**, *2*, 3518–3523. (d) Semenova, T. D.; Krasnykh, O. P. *Russ. J. Org. Chem.* **2005**, *41*, 1222–1227.

(34) (a) Ziegler, E.; Sterk, H. *Monatsh. Chem.* **1968**, *99*, 1958–1961. (b) Zhou, C.; Birney, D. M. *J. Org. Chem.* **2004**, *69*, 86–94.

SCHEME 11. Mechanistic Proposal for the Conversion 8 → 29 + 30 + 31

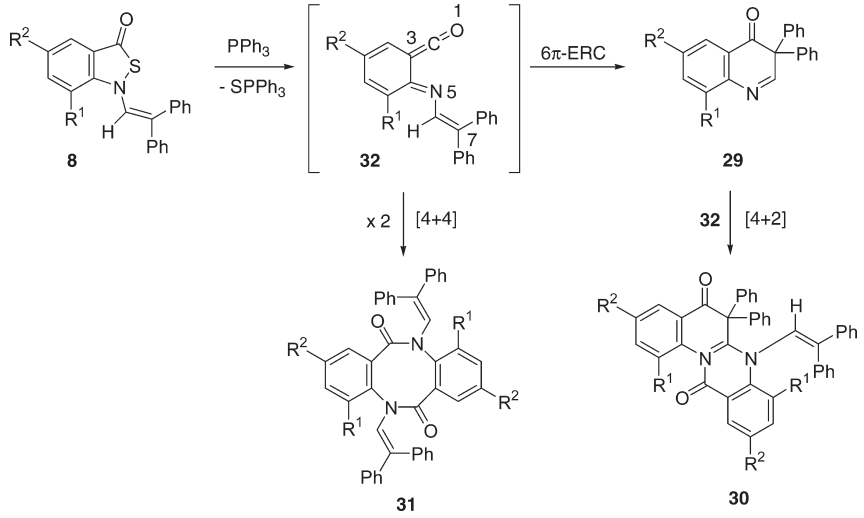

32b, which contributes to increase the population of its optimal reactive conformation for accomplishing the 6π electrocyclization step leading to quinolone **29b**. At the same time, this methyl group seems to make difficult the [4 + 2] cycloaddition of **32b** with a molecule of quinolone **29b** and the [4 + 4] cyclodimerization process.

With the aim of probing the participation of imidoylketenes **28** as reactive intermediates in the conversions **8** → **29/30/31**, we carried out the treatment of 2,1-benzisothiazol-3-one **8c** with triphenylphosphine using anhydrous ethanol as solvent (Scheme 12). This reaction provided, as the major product, the ethyl anthranilate **33** (31%), accompanied by the dibenzodiazocinedione **31c** (15%). The formation of anthranilate **33** seems to confirm that the desulfurization of compounds **8c** takes place via the imidoyl-ketene **32c**, which is then captured by the solvent through a nucleophilic addition at the ketene carbon atom, also undergoing, in a lesser extent, the cyclodimerization leading to **31c**.

Conclusions

In conclusion, we have disclosed a general fragmentation of 1,3-oxathiolane-ketenimines and -carbodiimides yielding the corresponding *N*-substituted 2,1-benzisothiazol-3-ones plus ethylene, and unveiled its mechanism by means of a computational DFT study. The tandem sequence of chemical events is composed of a 1,5-hydride shift, activated by the oxathiolane fragment, and a rare step of pseudopericyclic characteristics combining a 1,5-S,N-cyclization and the fragmentation of the oxathiolane ring in the transient *o*-azaxylylene intermediates. The results of the computations also agree with the observed reactivity order ketenimine > carbodiimide, discard alternative reaction channels, and fully explain the experimental outcomes of this work. Sulfur extrusion from the prepared benzisothiazolones by the action of triphenylphosphine is shown to provide three different classes of complex heterocycles whose relative ratio varies with the reaction conditions.

Experimental Section

For the preparation of 2-(2-azidophenyl)-1,3-oxathiolanes **5** and 2-(2-triphenylphosphoranylideneaminophenyl)-1,3-oxathiolanes **6**, see ref 8.

SCHEME 12. Desulfurization of 8c in Ethanol as Solvent

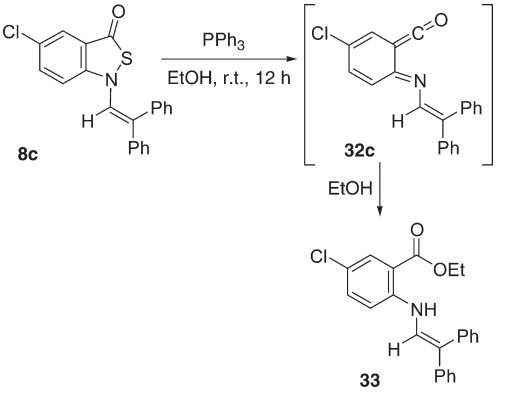

Procedure for the Preparation of the 2,1-Benzisothiazol-3-ones 8. To a solution of the corresponding 2-(2-triphenylphosphoranylideneaminophenyl)-1,3-oxathiolane **6** (1 mmol) in anhydrous toluene (15 mL) was added methylphenylketene (0.13 g, 1 mmol) or diphenylketene (0.19 g, 1 mmol) in the same solvent (5 mL). The reaction mixture was first stirred at room temperature for 15 min and then at reflux temperature for 1−7 h. After cooling, the solvent was removed under reduced pressure, and the resulting material was purified by column chromatography on silica gel, using hexanes/diethyl ether as eluent.

1-(2,2-Diphenylethenyl)-2,1-benzisothiazol-3(1*H*)-one 8a: eluent for column chromatography, hexanes/diethyl ether (9:1, v/v); yield 73%; mp 142 °C (yellow prisms, diethyl ether); IR (Nujol) 1663 (vs), 1625 (s) cm^{-1}; ^1H NMR ($CDCl_3$, 400 MHz) δ 7.01−7.05 (m, 1 H), 7.03 (s, 1 H), 7.16−7.21 (m, 2 H), 7.22−7.26 (m, 6 H), 7.28−7.31 (m, 3 H), 7.49 (ddd, 1 H, J = 8.4, 7.0, 1.4 Hz), 7.70 (dd, 1 H, J = 8.0, 0.7 Hz); ^{13}C NMR ($CDCl_3$, 100 MHz) δ 113.1, 121.3 (s), 121.4, 123.1, 124.1, 127.8, 128.0, 128.5, 128.7, 128.8, 131.0, 133.4 (s), 134.3, 136.8 (s), 140.2 (s), 152.1 (s), 189.5 (s); MS (EI, 70 eV) *m*/*z* (rel int) 329 (M^+, 96), 165 (100). Anal. Calcd for $C_{21}H_{15}NOS$ (329.42): C, 76.57; H, 4.59; N, 4.25. Found: C, 76.44; H, 4.44, N, 4.21.

Procedure for the Preparation of the 2,1-Benzisothiazol-3-ones 11. To a solution of the 2-(2-triphenylphosphoranylideneaminophenyl)-1,3-oxathiolane **6** (1 mmol) in anhydrous dichloromethane (20 mL) was added a solution of the aryl isocyanate (1 mmol) in the same solvent (5 mL). The reaction mixture was stirred at room temperature for 30 min. The solvent was

removed under reduced pressure, and the oily residue was chromatographed on a silica gel column using hexanes/diethyl ether (9:1, v/v) as eluent to give pure carbodiimides **10**.

A solution of the carbodiimide **10** (0.5 mmol) in anhydrous *o*-xylene (20 mL) was heated a 160 °C, in a sealed tube, for 24 h. The solvent was removed under reduced pressure, and the resulting material was purified by silica gel column chromatography using hexanes/diethyl ether as eluent.

(*E*)-1-[(4-Methylphenylimino)methyl]-2,1-benzisothiazol-3(*1H*)-one 11a: eluent for column chromatography, hexanes/diethyl ether (1:9, v/v); yield 51%; mp 144−145 °C (colorless prisms, diethyl ether); IR (Nujol) 1689 (vs), 1612 (s) cm^{-1}; ^1H NMR ($CDCl_3$, 300 MHz) δ 2.44 (s, 3 H), 7.26−7.36 (m, 4 H), 7.52−7.57 (m, 1 H), 7.75−7.83 (m, 2 H), 8.11 (s, 1 H), 8.36−8.38 (m, 1 H); ^{13}C NMR ($CDCl_3$, 75 MHz) δ 21.3, 122.5 (s), 126.8, 127.3, 127.6, 130.3, 134.6, 135.0 (s), 139.3 (s), 146.4, 148.0 (s), 161.0 (s). MS (EI, 70 eV) *m*/*z* (rel int) 236 (M^+ - 32, 100). Anal. Calcd for $C_{15}H_{12}N_2OS$ (268.34): C, 67.14; H, 4,51; N, 10.44. Found: C, 66.89; H, 4.27; N, 10.17.

Procedure for the Desulfurization of 2,1-Benzisothiazol-3-ones 8. Method A. A mixture of the 2,1-benzisothiazol-3-one **8** (1 mmol) and triphenylphosphine (1 mmol) was heated at 160 °C, in a sealed tube, for 1−4 h. After being cooled at room temperature, the crude material was purified by silica gel column chromatography using hexanes/diethyl ether as eluent.

Method B. A solution of the 2,1-benzisothiazol-3-one (1 mmol) and triphenylphosphine (1 mmol) in anhydrous toluene was stirred at room temperature for 12 h. The solvent was then removed under reduced pressure, and the resulting material was purified by silica gel column chromatography using hexanes/diethyl ether as eluent.

3,3-Diphenyl-4(3*H*)-quinolone 29a: eluent for column chromatography, hexanes/diethyl ether (1:1, v/v); yield 27%; mp 96−98 °C (colorless prisms, diethyl ether); IR (Nujol) 1672 (s) cm^{-1}; ^1H NMR ($CDCl_3$, 300 MHz) δ 7.12−7.46 (m, 11 H), 7.63−7.66 (m, 1 H), 7.69−7.75 (m, 1 H), 8.06−8.09 (m, 1 H), 8.37 (s, 1 H); ^{13}C NMR ($CDCl_3$, 75 MHz) δ 65.0 (s), 123.7 (s), 126.7, 128.3, 129.0, 129.1, 129.2, 129.3, 136.3, 138.6 (s), 146.8 (s), 168.9, 195.9 (s); MS (EI, 70 eV) *m*/*z* (rel int) 297 (M^+, 100). Anal. Calcd for $C_{21}H_{15}NO$ (297.36): C, 84.82; H, 5.08; N, 4.71. Found: C, 84.43; H, 4.99; N, 4.88.

Quinolino[2,1-*b*]quinazolin-5,12-dione 30a: eluent for column chromatography, hexanes/diethyl ether (1:1, v/v); yield 60%; mp 222−223 °C (colorless prisms, diethyl ether); IR (Nujol) 1674 (s) cm^{-1}; ^1H NMR ($CDCl_3$, 400 MHz) δ 6.30 (s, 1 H), 6.49 (s, 1 H), 6.56 (t, 1 H, J = 7.3 Hz), 6.66 (d, 1 H, J = 8.3 Hz), 6.85−6.91 (m, 4 H), 6.97−7.03 (m, 3 H), 7.14−7.32 (m, 10 H), 7.34−7.39 (m, 6 H), 7.45 (d, 1 H, J = 8.1 Hz), 7.54−7.58 (m, 1 H), 7.90 (dd, 1 H, J = 8.1, 1.3 Hz); ^{13}C NMR ($CDCl_3$, 100 MHz) δ 70.6 (s), 78.0, 112.1, 114.7 (s), 118.5, 125.7, 126.4, 127.5, 127.6, 128.1, 128.2, 128.3, 128.4, 128.5, 128.8, 129.2, 130.2, 131.6, 133.9, 134.0, 134.8 (s), 137.4 (s), 137.7 (s), 138.5 (s), 139.6 (s), 142.5 (s), 146.6 (s), 160.9 (s), 197.7 (s); MS (EI, 70 eV) *m*/*z* (rel int) 594 (M^+, 70), 297 (100). Anal. Calcd for $C_{42}H_{30}N_2O_2$ (594.71): C, 84.82; H, 5.08; N, 4.71. Found: C, 84.96; H, 5.30; N, 4.92.

Dibenzo[*b*,*f*][1,5]diazocin-6,12-dione 31c: eluent for column chromatography, hexanes/diethyl ether (9:1, v/v); yield 53%; mp 171−172 °C (colorless prisms, diethyl ether); IR (Nujol) 1632 (s) cm^{-1}; ^1H NMR ($CDCl_3$, 400 MHz) δ 7.06 (d, 2 H, J = 11.2 Hz), 7.11 (d, 2 H, J = 9.2 Hz), 7.19−7.33 (m, 14 H), 7.39−7.43 (m, 6 H), 7.77 (d, 2 H, J = 2.4 Hz), 9.71 (d, 2 H, J = 11.2 Hz); ^{13}C NMR ($CDCl_3$, 100 MHz) δ 110.7 (s), 114.3, 121.9, 122.3 (s), 123.9 (s), 126.6, 126.9, 127.8, 128.5, 129.2, 130.0, 131.5, 136.4, 137.5 (s), 141.2 (s), 145.6 (s), 162.7 (s); MS (EI, 70 eV) *m*/*z* (rel int) 666 (M^+ + 4, 3), 664 (M^+ + 2, 16), 662 (M^+, 25), 165 (100). Anal. Calcd for $C_{42}H_{28}Cl_2N_2O_2$ (663.60): C, 76.02; H, 4.25; N, 4.22. Found: C, 76.35; H, 4.12; N, 4.51.

Computational Methods

All calculations were carried out in the gas phase with the Gaussian03[35] suite of programs. An intensive characterization of the potential energy surface was done at the HF/6-31G*[36] theoretical level and then with the hybrid three-parameter functional customarily denoted as B3LYP[37] using the 6-31+G** basis set. All of the reported stationary points were fully optimized by analytical gradient techniques. To check the accuracy and performance of the B3LYP functional in the study of these transformations we have also optimized the molecular geometries of all the stationary points found in the potential energy surface associated to the conversion **20a** →**21a**/**22a** and **20a′** →**21a′** using the new hybrid meta exchange correlation functional M06 of Truhlar and Zhao,[38] with the internal 6-31+G** basis set, and the values obtained for the energy barriers and reaction energies are very similar to the values based on B3LYP geometries (see the Supporting Information). Harmonic frequency calculations at each level of theory verified the identity of each stationary point as a minimum or a transition state and were used to provide an estimation of the zero-point vibrational energies (ZPVE), which were not scaled. The intrinsic reaction coordinates (IRC)[39] were followed to verify the energy profiles connecting each transition state to the correct local minima by using the second-order Gonzalez−Schlegel integration method.[40] Natural charges and second order perturbation analyses were evaluated using the natural bond orbital (NBO) method.[22] To assess the possible biradical character of the species involved in these conversions CASSCF[41](6,6)/6-31G*//B3LYP/6-31+G** calculations of all the stationary points found in the transformation **20a** →**21a**/**22a** were performed. The results show that the closed-shell S0 wave function is largely the predominant one (94−97%). Therefore, we can conclude that these structures are adequately described with a single reference wave function.

Acknowledgment. This work was supported by the Ministerio de Ciencia e Innovacion of Spain (Project

(35) Frisch, M. J.; Trucks, G. W.; Schlegel, H. B.; Scuseria, G. E.; Robb, M. A.; Cheeseman, J. R.; Montgomery, J. A., Jr.; Vreven, T.; Kudin, K. N.; Burant, J. C.; Millam, J. M.; Iyengar, S. S.; Tomasi, J.; Barone, V.; Mennucci, B.; Cossi, M.; Scalmani, G.; Rega, N.; Petersson, G. A.; Nakatsuji, H.; Hada, M.; Ehara, M.; Toyota, K.; Fukuda, R.; Hasegawa, J.; Ishida, M.; Nakajima, T.; Honda, Y.; Kitao, O.; Nakai, H.; Klene, M.; Li, X.; Knox, J. E.; Hratchian, H. P.; Cross, J. B.; Adamo, C.; Jaramillo, J.; Gomperts, R.; Stratmann, R. E.; Yazyev, O.; Austin, A. J.; Cammi, R.; Pomelli, C.; Ochterski, J. W.; Ayala, P. Y.; Morokuma, K.; Voth, G. A.; Salvador, P.; Dannenberg, J. J.; Zakrzewski, V. G.; Dapprich, S.; Daniels, A. D.; Strain, M. C.; Farkas, O.; Malick, D. K.; Rabuck, A. D.; Raghavachari, K.; Foresman, J. B.; Ortiz, J. V.; Cui, Q.; Baboul, A. G.; Clifford, S.; Cioslowski, J.; Stefanov, B. B.; Liu, G.; Liashenko, A.; Piskorz, P.; Komaromi, L.; Martin, R. L.; Fox, D. J.; Keith, T.; Al-Laham, M. A.; Peng, C. Y.; Nanayakkara, A.; Challacombe, M. P.; Gill, M. W.; Johnson, B. G.; Chen, W.; Wong, M. W.; Gonzalez, C.; Pople, J. A. *Gaussian 03*, Revision B.03; Gaussian, Inc.: Pittsburgh, PA, 2003.

(36) Hehre, W. J.; Radom, L.; Schleyer, P. v. R.; Pople, J. A. In *Ab Initio Molecular Orbital Theory*; Wiley: New York, 1986; pp 71−82 and references cited therein.

(37) (a) Parr, R. G.; Yang, W. *Density-Functional Theory of Atoms and Molecules*; Oxford University Press: New York, 1989. (b) Bartolotti, L. J.; Fluchichk, K. In *Reviews in Computational Chemistry*; Lipkowitz, K. B., Boyds, D. B., Eds.; VCH Publishers: New York, 1996; Vol. 7; pp 187−216. (c) Kohn, W.; Becke, A. D.; Parr, R. G. *J. Phys. Chem.* **1996**, *100*, 12974–12980. (d) Ziegler, T. *Chem. Rev.* **1991**, *91*, 651–667.

(38) Zhao, Y.; Truhlar, D. G. *Theor. Chem. Acc.* **2008**, *120*, 215–241. Zhao, Y.; Truhlar, D. G. *Acc. Chem. Res.* **2008**, *41*, 157–167.

(39) (a) Fukui, K. *J. Phys. Chem.* **1970**, *74*, 4161–4162. (b) Fukui, K. *Acc. Chem. Res.* **1981**, *14*, 363–368.

(40) (a) Gonzalez, C.; Schlegel, H. B. *J. Phys. Chem.* **1990**, *94*, 5523–5527. (b) Gonzalez, C.; Schlegel, H. B. *J. Chem. Phys.* **1991**, *95*, 5853–5860.

(41) (a) Hegarty, D.; Robb, M. A. *Mol. Phys.* **1979**, *38*, 1795–1812. (b) Eade, R. H. E.; Robb, M. A. *Chem. Phys. Lett.* **1981**, *83*, 362–368. (c) Schlegel, H. B.; Robb, M. A. *Chem. Phys. Lett.* **1982**, *93*, 43–46.

CTQ2008-05827/BQU) and Fundacion Seneca-CARM (Project 08661/PI/08). B.B. also thanks Fundacion Seneca-CARM for a fellowship.

Supporting Information Available: Spectral data (NMR, IR, MS, and elemental analyses) for compounds **8b**−**e**, **11b**−**c**, **29b**,**d**, **30d**, **31d**, and **33**. ^{1}H and ^{13}C NMR spectra of compounds **8**, **11**, **29**−**31**, and **33**. Details of computational procedures, Cartesian coordinates, and energies for all the stationary points. This material is available free of charge via the Internet at http://pubs.acs.org.